ORIGINAL PAPER

Assessment of relative active tectonics in parts of Aravalli mountain range, India: implication of geomorphic indices, remote sensing, and GIS

Syed Ahmad Ali[1] · Javed Ikbal[1]

Abstract
Udaipur is located in the southern front of NE-SW oriented Aravalli hills. The area is dissected by several active fault/lineaments. To access the tectonic scenario, we have used a widely used conventional geomorphic indices such as stream length-gradient index (SL), asymmetry factor (Af), basin shape (Bs), valley floor width to valley height ratio (Vf), mountain front sinuosity (Smf), hypsometric integral (Hi), hypsometric curve, and transverse topographic symmetry factor (T) to analyze relative index of active tectonics (RIAT) of the Ahar watershed. Results of these geomorphic indices of each sub-watersheds are used to divide area from low to high tectonic activity classes. The results of relative index of active tectonic (RIAT) distribution pattern shows that the sub-watershed UDSW2, 3, and 4 is tectonically relatively more tectonically active than the other parts of the study area. The estimated results of RIAT distribution are well supported by the geomorphic evidences. The combined results of geomorphic evidences such as stream deflection and analysis of lineament and geomorphic indices reveal that the Ahar watershed of Udaipur district is most affected by tectonic activity.

Keywords Geomorphic indices · Relative active tectonics · Stream deflection · Lineament · Aravalli mountain range

Introduction

Tectonic geomorphology is one of the emergent disciplines in geosciences due to the advent of novel geomorphological, geodetic, and geochronological tools which aid the acquisition of rates (uplift rates, incision rates, erosion rates, slip rates on faults, etc.) at variable timescales (10^3–10^6 years) (Burbank and Anderson 2001; Azor and Keller 2002; Bull 2007, Ali and Ali 2018; Whipple et al. 2013; Whittaker 2012; Kothyari 2015; Kothyari et al. 2016a). This discipline is important because the results of regional studies on neotectonics are significant for evaluating natural hazards, land use development, and management in populated areas (Pedrera et al. 2009; Joshi

✉ Syed Ahmad Ali
ahmadali.syed@gmail.com

Javed Ikbal
jvdikbal@gmail.com

[1] Department of Geology, Aligarh Muslim University, Aligarh 202002, India

et al. 2013; Dubey et al. 2017). The study of geomorphology, structural geology, stratigraphy, geochronology, seismology, and geodesy may assist in understanding the landscape evolution and recognize active tectonic movements (Riquelmea et al. 2003; Malik and Mohanty 2007; Bathrellos et al. 2009; Kamberis et al. 2012; Kothyari et al. 2016a). Tectonically active region influenced on drainage pattern, basin asymmetry, stream deflection, river incision (Cox 1994). The geomorphic indices are important indicators capable of decoding landform responses to active deformation processes and have been widely used as a reconnaissance tool to differentiate zones deformed by active tectonics (Keller and Pinter 1996; Chen et al. 2003). The quantitative measurements of landforms are accomplished on the basis of calculation of geomorphic indices by the use of topography maps, digital elevation model satellite images, aerial photographs, and field works (Schum 1977; Toudeshki and Arian 2011; Ahmad and Bhat 2013; Ikbal and Ali 2017; Ikbal et al. 2017).

Geomorphic indices of active tectonics have been developed as basic reconnaissance tools to recognize areas experiencing rapid tectonic deformation (Bull and McFadden 1977). The quantitative measurement of landscape is based on the calculation of geomorphic indices using different data sources. These

geomorphic indices at regional scale provide basic reconnaissance tools to identify tectonically active regions (Keller 1986), their susceptibility to tectonic deformation, and level of tectonic activity (Keller and Pinter 1996; Demoulin 1998). Geomorphic indices of active tectonics are known to be helpful in assessing active tectonics (Bull and McFadden 1977; Keller and Pinter 1996; Azor and Keller 2002; Silva et al. 2003; Molin et al. 2004; Gaidzik and Ramírez-Herrera 2017) and are computed in the present study. Intra-continental deformation within Indian plate took place due to collision between Indian and Eurasian plate (Bhu et al. 2014). Release of strain along major faults within stable craton is responsible for intra-continental deformation (Roy and Jakhar 2002). Bhu et al. (2014) have marked the epicenters of low magnitude (< 5) which are located on the Precambrian lineaments as well as NW-SE striking younger lineaments reveals the rejuvenation of Precambrian lineament and younger lineament due to neotectonic activity. The Global Positioning System (GPS) measurements of 2007–2011 suggest that the Udaipur block moves at a rate of about 49 mm/year towards northeast (Bhu et al. 2014), also indicating tectonically active area. The study area is located in the northern part of Udaipur district of Rajasthan (Fig. 1a). Udaipur city is a world famous tourist place. Various historical monuments are seen there. The tourism has a great influence on economy of that area. To attract tourists, the area should be developed, and for the development, it is necessary to study about neotectonic activity of the particular area. The main Ahar river passes through this region therefore morphotectonic study of Ahar watershed has been attempted. Each of the following six geomorphic indices include basin asymmetry factor (Af), basin shape index (Bs), hypsometric integral (Hi) and curve, the stream length-gradient index (SL), mountain-front sinuosity (Smf), and valley floor width to valley height ratio (Vf) were applied to assess the relative tectonic activity.

Generalized geology and tectonics

The study area consists of Precambrian rocks of Aravalli Supergroup. A thick deposits of quaternary sediments also observed along major river valleys of the eastern and southern Rajasthan (Roy and Jakhar 2002). The Banded Gneissic Complex of Precambrian age is considered as the basement over which Proterozoic rock (Aravalli and Delhi Supergroup) were deposited (Heron 1936). The oldest formation exposed in the area belongs to Bhilwara Supergroup (Banded Gneissic Complex) of Arachean age. The younger formations of Aravalli Supergroup and Delhi Supergroup of Proterozoic age is found in the western side of the study area. Aravalli Supergroup consists of Debari group, Udaipur group, Bari lake group, and Jharol group (Ali et al. 2017). Lithologically metavolcanics, conglomerate, dolomite, phyllite, quartzite, mica schist are present in Debari group whereas Udaipur group is composed of phyllite, metagreywacke, metaconglomerate, and quartzite (Ikbal 2018). Bari lake group, overlain by Udaipur group, is composed of pebbly arkose, quartzite, metaconglomerate, dolomite, and Jharol group which is overlain by Bari lake group composed of quartzite, phyllite, chlorite schist, and mica schist (Ikbal 2018).

This region was an active zone of sedimentation, distinct tectonism, and repetitive magmatism during the end of Mesozoic (Bakliwal and Ramasamy 1987). Bhilwara belt and the Udaipur-Jharol belt are two major adjoining belts situated in
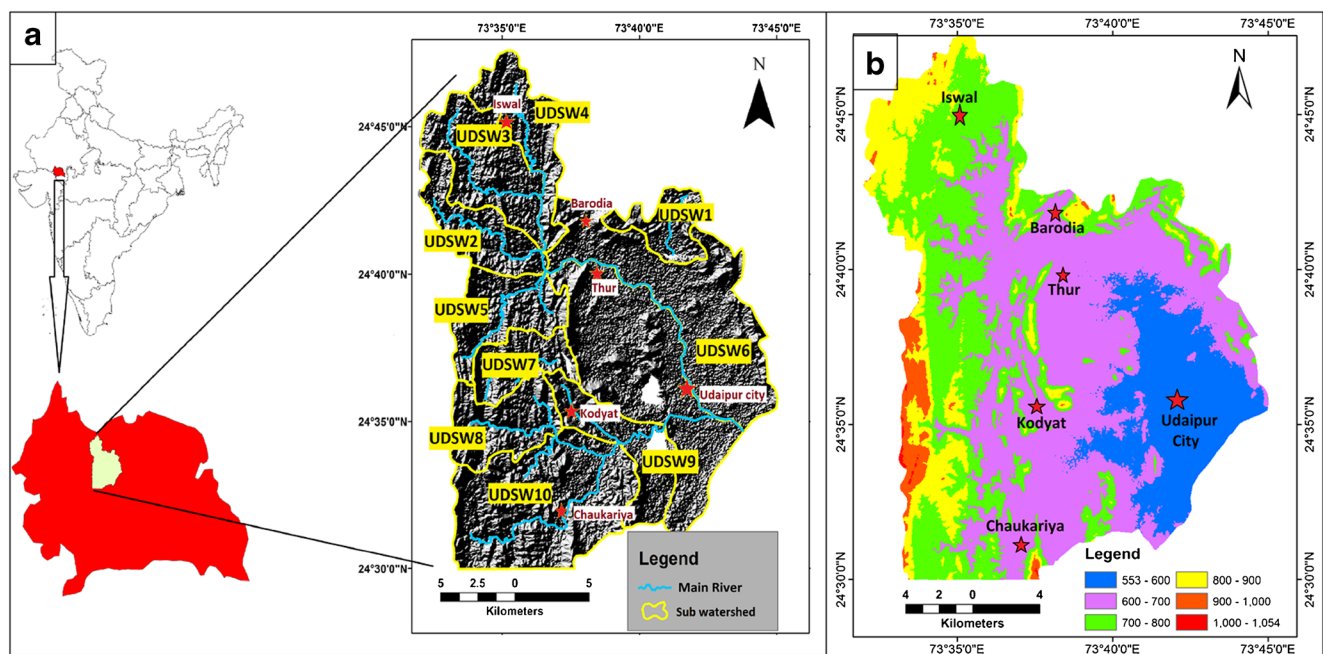

Fig. 1 (a) Location map of the study area, (b) elevation map

Aravalli Supergroup. The Udaipur-Jharol belt is exposed as an inverted "V"-shaped area with tapering end near Nathdwara. Rakhabdev lineament, which divide this belt, symmetrically trends N-S. The major lineaments which passes through the area are (I) Udaipur-Sandarpur lineament forming the contact between Debari and Udaipur group of rocks, trending NW-SE (Bakliwal and Ramasamy 1987), (II) Rakhabdev lineament, trending N-S intersect older and younger sequence of Aravalli Supergroup, indicating its reactivation during Proterozoic and Cenozoic age(Bakliwal and Ramasamy 1987), (III) Chambal-Jamnagar lineament trending NE-SW, crosscut Rakhabdev lineament (Bakliwal and Ramasamy 1987), and (IV) Darwal to Jogiwan lineament traverses parallel to Rakhabdev lineament through eastern contact of Balicha formation of Udaipur group, and morphotectonically it is defined by the angular discordance in the structural trends on the two sides of the lineament(Saifuddin 2000). Geological map with faults and major lineaments are shown in Fig. 2.

Geomorphology

According to the report of CGWB (201403), the geomorphology of Ahar watershed is divided into four geomorphic units such as structural hill, pediment, buried pediment, and valley fill. The report gave detail information about the above geomorphic units. Structural hills are found in the western part of the study area. Linear to arcuate hills is showing definite trend lines with varying lithology associated with faulting and folding. Valley fill is formed due to fluvial activity found at lower topographic location (in between structural hills) composed of boulders, cobbles, pebbles, gravels, sand, silt, and clay. The unit has consolidated sediment deposit. Pediment and buried pediment are denudational origin found southwest and eastern part of the study area and scattered in entire Udaipur district. Pediment is broad gently sloping rock flooring, erosional surface, comprising varied lithology, whereas buried pediment covers essentially with relatively thicker alluvial, colluvial weathered material.

Methodology

Remote sensing and GIS are valuable tools and used worldwide to understand terrain characteristics in terms of geomorphology, tectonics, structural study, and so on. Field study of large area is difficult. However remote sensing and GIS make
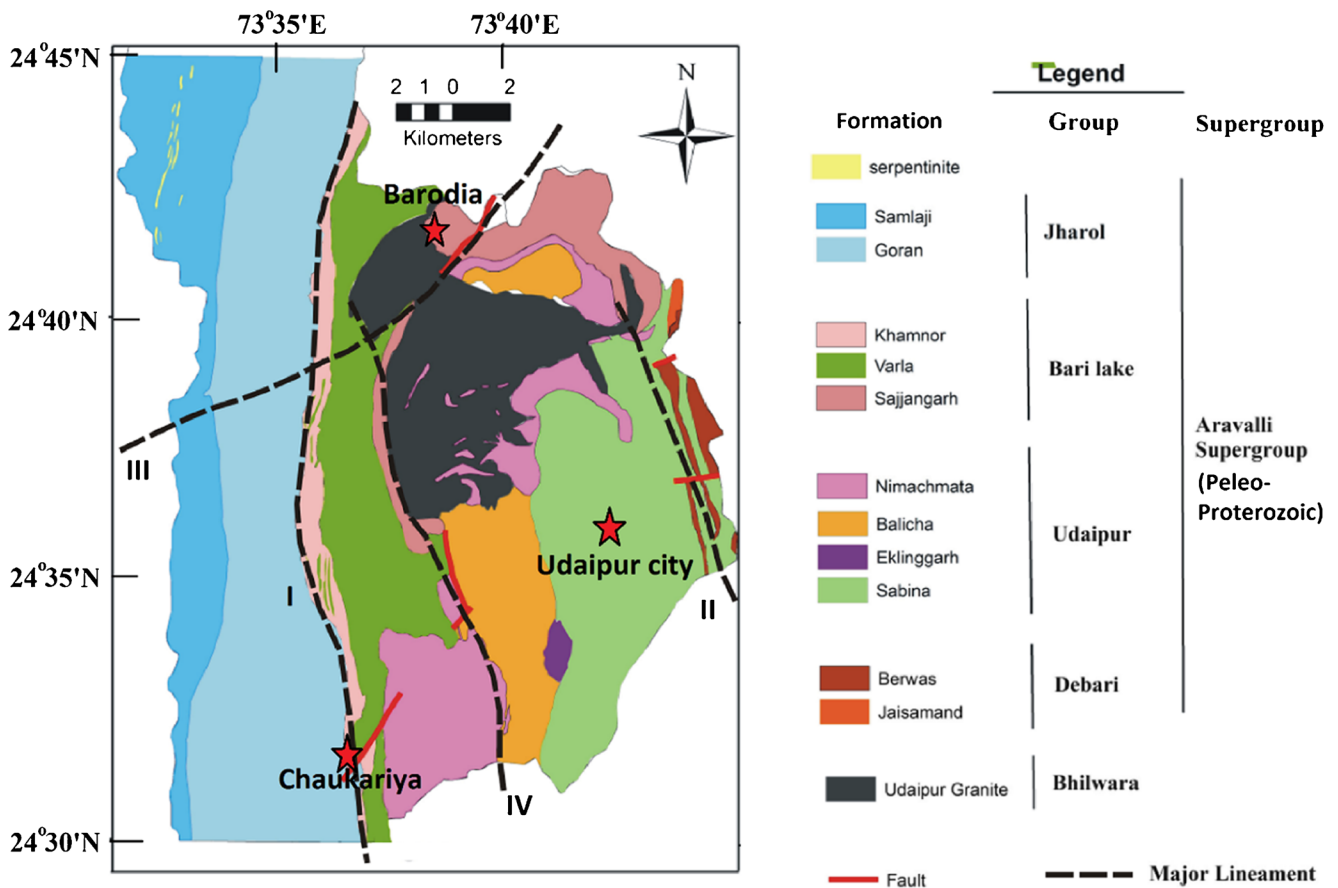

Fig. 2 Geological map of the study area (Geological Survey of India), (I) Rakhabdev lineament, (II) Udaipur-Sandarpur lineament, (III) Chambal-Jamnagar lineament, (IV) Darwal-Jogiwan lineament

it possible and save time. Stream network and watershed boundary was delineated using SRTM (30 m) under GIS environment. For extracting drainage network, river has been defined by applying river threshold number of 500 that is the number of cells to start a river. Laplacian, sobel, false color composite image were created by using Landsat ETM+ (2008), and shaded relief map was prepared by SRTM DEM to recognize linear features. Satellite image has been processed for edge enhancement by ERDAS IMAGINE 14 software to recognize linear geological features. Steep slope or abrupt changes in slope of terrain is most likely a fault scarp or active faulting although edges of plateau, stream banks, road cuts, etc. provides steep slope. In comparison of two-dimensional satellite data, using three-dimensional digital elevation model is easy to detect positive lineaments (topographic high) as well as negative lineaments (topographic low). The geomorphic indices such as stream length gradient index (SL), valley floor width to valley height ratio (Vf), hypsometric integral (Hi), mountain front sinuosity (Smf), asymmetry factor (Af), basin shape (Bs), and transverse topographic symmetry factor (T) (Table 1) were calculated using SRTM DEM. SL value was calculated by given formula (Table 1) where dH is difference of elevation between two points, dL is the length of this stretch, and L is the total length of the channel. The value of SL index over the study area was calculated along the master stream of 10 sub-watersheds. The values of maximum, minimum, and mean elevation are directly taken from DEM by arc GIS software. To check out the accuracy of the values particularly mean elevation data point sampling of more than 100 elevation values were collected from every sub-watershed and computed by using DEM. The value of Smf was computed by dividing Lmf (measured the length of the mountain front along the foot of the mountain) by Ls (the value of straight line length of that particular front). Frontal side of the mountain with more than 800 m in elevation and contour interval between top of the hill or mountain and piedmont are more than 300 m and have been considered as mountain front to analyze mountain front sinuosity. For the study of asymmetry factor (Af), A_r (area of the right side of the master stream) and A_t (total area of the watershed) was measured by Arc Map and to calculate these parameter,

looking downstream of master streams of every sub-watershed was considered. As the value of width of sub-watershed vary in place to place, so average value was taken to calculate basin shape. A number of segments in each sub-watershed have been considered to determine TTSF value, and average value is taken to understand asymmetrical behavior of sub-watershed. After calculating the above geomorphic indices, every sub-watershed has been classified into three classes based on the index value. Relative index of active tectonics (RIAT) is obtained by the average of the different classes of geomorphic indices (S/n) and divided into four classes according to their relative tectonic activity. Stream deflection parameter, lineament map, and field evidences were used to support the result come from the analysis of above geomorphic indices.

Results and discussion

Analysis of geomorphic indices

Stream length gradient index (SL)

Relative tectonic activity of an area can be appraised by using SL index. Deviation from this stable river profile may be induced by tectonic, lithological, and/or climatic factors (Hack 1973). Soft rocks comprising high SL values is the indicators of recent tectonic activity, but low values of SL in the area encompasses strike slip faults and streams are flowing through it may also represent tectonically active (Keller and Pinter 1996; Mahmood and Gloaguen 2012). Rocks of consistent resistance showing high value of stream length gradient index or fluctuation of SL values indicates the area is tectonically active (Keller 1986). The SL values were classified into three classes, where SL values more than 600 falls in class 1, SL value in between 300 and 600 fall in class 2, and in class 3, the values of SL is less than 300 (El Hamdouni et al. 2008).

The average value of all the sub-watersheds are below 300 and fall in class 3 (Table 2). Relative study shows that sub-watershed UDSW2, UDSW3, and UDSW4 shows relatively higher SL value, i.e., more than 200, followed by UDSW5 and

Table 1   Formula of different geomorphic indices

Parameter	Formula	References
Stream length gradient index (SL)	SL = (dH/dL)*L	Hack 1973
Ratio of valley floor to valley height (Vf)	Vf = 2Vfw/ [(Eld − Esc) + (Erd − Esc)]	Bull 1977, 1978
Hypsometry integral (HI)	HI = (Elev $_{mean}$ − Elev $_{min}$)/(Elev $_{max}$ − Elev $_{min}$)	Pike and Wilson 1971
Mountain front sinuosity (Smf)	Smf = Lmf/Ls	Bull and McFadden 1977
Asymmetry factor	AF = (A_r/A_t) × 100	Hare and Gardner 1985
Basin shape (Bs)	Bs = Bl/Bw	Bull and McFadden 1977
Transverse topographic symmetry factor (T)	T = Da/Dd	Cox 1994

UDSW8 which are relatively moderate SL value and the value ranges between 100 and 200, remaining sub-watersheds show low SL value, i.e., less than 100 (Fig. 5a). The relative value indicates that northern and western part of the Ahar watershed shows relatively high and moderate tectonically active respectively. Eastern, southern, and central part is relatively tectonically less active. Places were marked where SL value relatively high and this high value may be due tectonically uplifted or diverse erosion (Fig. 3).

Ratio of valley floor width to valley height (Vf)

The Vf index reflects the difference between V-shaped valleys that are down cut in response to active uplift (low values of Vf) and broad-floored valleys that are eroding laterally into adjacent hill slopes in response to base-level stability (high values of Vf) (Bull 1978). Deep V-shaped valleys (Vf < 1) are connected with linear, active downcutting streams distinctive of areas subjected to active uplift, while flat floored (U-shaped) valleys (Vf > 1) show an attainment of the base level of erosion mainly in response to relative tectonic quiescence (Keller 1986).

Different researcher classified Vf index with different values (El Hamdouni et al. 2008; Mahmood and Gloaguen 2012). Master stream of sub-watersheds were used to calculate the Vf values of the study area. In this study area, Vf index is classified as Class 1 (Vf < 0.5), Class 2 (0.5 ≤ Vf < 1), and Class 3 (Vf ≥ 1) (El Hamdouni et al. 2008). Although the average Vf value of all the sub-watersheds in the study area is more than 1 falling Class 3 indicating flat-floored U-shaped valley (Table 2), but in some places mainly along the lineaments, faults and mountainous region where Vf value is less than 1 indicating "V"-shaped valley.

Hypsometric curve and hypsometric integral (HI)

Hypsometric curve is the area-altitude relation that can be described as a proportion of area above each proportion in elevation. The hypsometric integral (HI) describes the relative distribution of elevation in a given area of a landscape particularly a drainage basin. The study of hypsometric curves as well as HI values provides an important information about tectonic behavior of the watershed along with erosional stage of the watershed (Moglen and Bras 1995; Willgoose 1998; Huang and Niemann 2006; Aldharab et al. 2018a, b). Convex-up curves having high value of HI are representing youthful stage, smooth s-shaped curves crossing the center of the diagram characterize mature stage, and concave-up with low HI values are indicator of old stage (Strahler 1952). Figure 4 shows the hypsometric curves of every sub-watersheds.

The value of HI index always ranges between 0 and 1 which is computed in number. On the basis of values and in respect of convexity and concavity of hypsometric curves, hypsometric integral can be classified into three classes such as class 1 (HI > 0.5) shows convex hypsometric curve, class 2 (0.4 < HI < 0.5) shows concavo-convex or straight curve, and class 3 (HI < 0.4) having the curve of concave shape. Generally high values of hypsometric integral show convex hypsometric curve, and low values are responsible for concave curve. Hypsometric integral is convex in the lower portion, or low elevated area may relate to uplift along a fault or perhaps uplift associated with recent folding (El Hamdouni et al. 2008). High values of the index are possibly related to young active tectonic, and low values are related to older landscapes that have been more eroded and less impacted by recent active tectonics. The HI value in the Ahar watershed ranges from 0.165 (UDSW9) to 0.461 (UDSW4) (Table 2). Based on hypsometric integral, sub-watershed has been classified into three classes (Fig. 5b). UDSW2, 3, 4, and 8 shows convex upward curve with high hypsometric integral value and the value ranges from 0.38 to 0.46 indicates active uplift and high river incision, whereas the remaining parts of the study area shows concave upward and low hypsometric integral.

Mountain front sinuosity (Smf)

Smf value can be computed through topographic map or aerial photography or satellite imagery and the obtain value depends on the scale of the map. Small-scale map produces approximate values of Smf, while large-scale topographic map and aerial photography have higher resolution and are more appropriate for assessment of Smf (El Hamdouni et al. 2008). Mountain front sinuosity is defined as the ratio of the length of the mountain front along the foot of the mountain to the straight line length of that front (Bull 2007; Mahmood and Gloaguen 2012). The balance between erosion that tends to produce asymmetrical or sinuous fronts and tectonic forces that tend to create a straight mountain front coincident with an active range – bounding fault is presented by the above mentioned index. On the basis of tectonically activeness, some researchers have classified this value with three classes. Some studies have proposed that Smf values lower than 1.4 are indicative of tectonically active fronts (Burbank and Anderson 2001; Rockwell et al. 1985; Keller 1986). The Smf values are classified into three classes; class 1 in which Smf < 1.1, class 2 in which 1.1 ≤ Smf < 1.5, and class 3 when Smf ≥ 1.5 (El Hamdouni et al. 2008). In the study area, Smf value lies between 1.08 and 2.73; here sub-watershed wise Smf value was consider. Instead of 1.08 of Smf value in UDSW2 which is very tectonically active and fall in class 1 (El Hamdouni et al. 2008), but UDSW2 has two mountain front and the average value is 1.11 (Table. 2) and this sub watershed fall in class 2. Mountain front sinuosity of UDSW1 and UDSW6 fall in class 3 indicates less active tectonic and UDSW 2, UDSW3, UDSW4, UDSW5, UDSW7

Table 2 Sub-watershed wise SL value with class

Sub-watershed	SL	Vf	HI	Smf	Avg. Smf	AF	AF-50	Bs	TTSF
UDSW1	78.67	1.5	0.27567568	2.73	2.03	54.38	4.38	1.51	0.18
				1.33					
UDSW2	232.6	1.92	0.4054878	1.14	1.11	59.59	9.59	4.07	0.42
				1.08					
UDSW3	232.54	1.90	0.44932432	1.44		42.83	− 7.17	3.07	0.41
UDSW4	238.81	1.68	0.46101695	1.42		36.93	− 13.07	4.71	0.47
UDSW5	132.19	1.74	0.336	1.19		49.16	− 0.84	1.95	0.47
UDSW6	27.52		0.17280453	1.60	1.65	51.78	1.78	1.95	0.32
				1.82					
				1.45					
				1.48					
				1.90					
UDSW7	77.96	3.77	0.2887538	1.25		41.57	−8.43	1.98	0.18
UDSW8	108.61	1.63	0.38321995			50.97	0.97	2.01	0.32
UDSW9	46.69	3.79	0.16519174			52.35	2.35	4.09	0.05
UDSW10	88.06	1.81	0.28162291	1.45	1.25	44.18	−5.82	1.67	0.41
				1.05					

,and UDSW10 shows tectonically moderately active (Table 2 and Fig. 5c). The Smf value of mountain front located lower most part of the sub-watershed UDSW10 is 1.05, and this low value is because this front is align along fault trace.

Asymmetry factor (Af)

Tectonic tilting with direction of tilting of drainage basin can be evaluated by the analysis of Asymmetry factor at the scale of drainage basin (Siddiqui 2014; Kele et al. 2014). Af significantly greater or smaller than 50 shows influence of either active tectonics or lithologic structural control or differential erosion, as for example, the stream slipping down bedding plains over time (Elias 2015). Inclination of schistocity or bedding allows for preferred migration of the valley in the down-dip direction, producing an asymmetric valley (El Hamdouni et al. 2008). The values of this index are divided into three categories. 1 ($Af < 35$ or $Af \geq 65$), 2 ($57 \leq Af < 65$) or ($35 \leq Af < 43$), and 3 ($43 \leq Af < 57$) (Elias 2015). Af value in the study area ranges from 36.93 (UDSW4) to 59.59 (UDSW2) (Table 2). Sub-watersheds UDSW2, UDSW3, UDSW4, and UDSW7 fall in class 2 and the Af values of these sub watersheds indicate moderate tilting in this area whereas the remaining areas fall in class 3 and show very slight tilting or no tilting. Af value more than 55 and less than 45 are consider as asymmetrical basin, while the value of Af in between 45 and 55 are considered as symmetric of the basin (Çağlar Özkaymak 2015).

In order to express the direction of tilting, we subtracted the AF value from 50. The AF-50 value is the difference between the AF value and tectonically neutral value of 50. After subtracting some negative and few positive values have come which indicated the direction of tilting. The positive value shows left side tilting-looking downstream, and negative value shows right side tilting-looking downstream. UDSW3, 4, 7, and 10 has the value of AF-50 is − 7.17, − 13.07, − 8.43, and − 5.82 respectively showing left side tilting, whereas UDSW2 has the value of 9.59 showing right side tilting (Fig. 5d). The value within + 5 and − 5 is considered the area that has suffered very less tilting or no tilting. Tectonic tilting of UDSW3 and UDSW4 are west to southwest direction, UDSW7 and UDSW10 towards southern direction, and UDSW2 and UDSW1 are towards northeastern and east direction, respectively.

Basin shape (Bs)

Drainage basins with elongated in shape indicate relatively young in nature in active tectonic areas. With continued evolution or less active tectonic processes, the elongated shape tends to evolve to a more circular shape (Bull and McFadden 1977). Bs index can be classified as Class 1 ($Bs \geq 4$), Class 2 ($3 \leq Bs \leq 4$), and class 3 ($Bs \leq 3$) (Elias 2015) (Fig 5e). High values of Bs are associated with elongated basins, generally associated with relatively higher tectonic activity and Low values of Bs indicate a more circular-shaped basin, generally associated with low tectonic activity (El Hamdouni et al. 2008).

Bs value ranges from 1.51 (UDSW1) to 4.71 (UDSW2) (Table 2). UDSW2, UDSW4, and UDSW9 have Bs index is
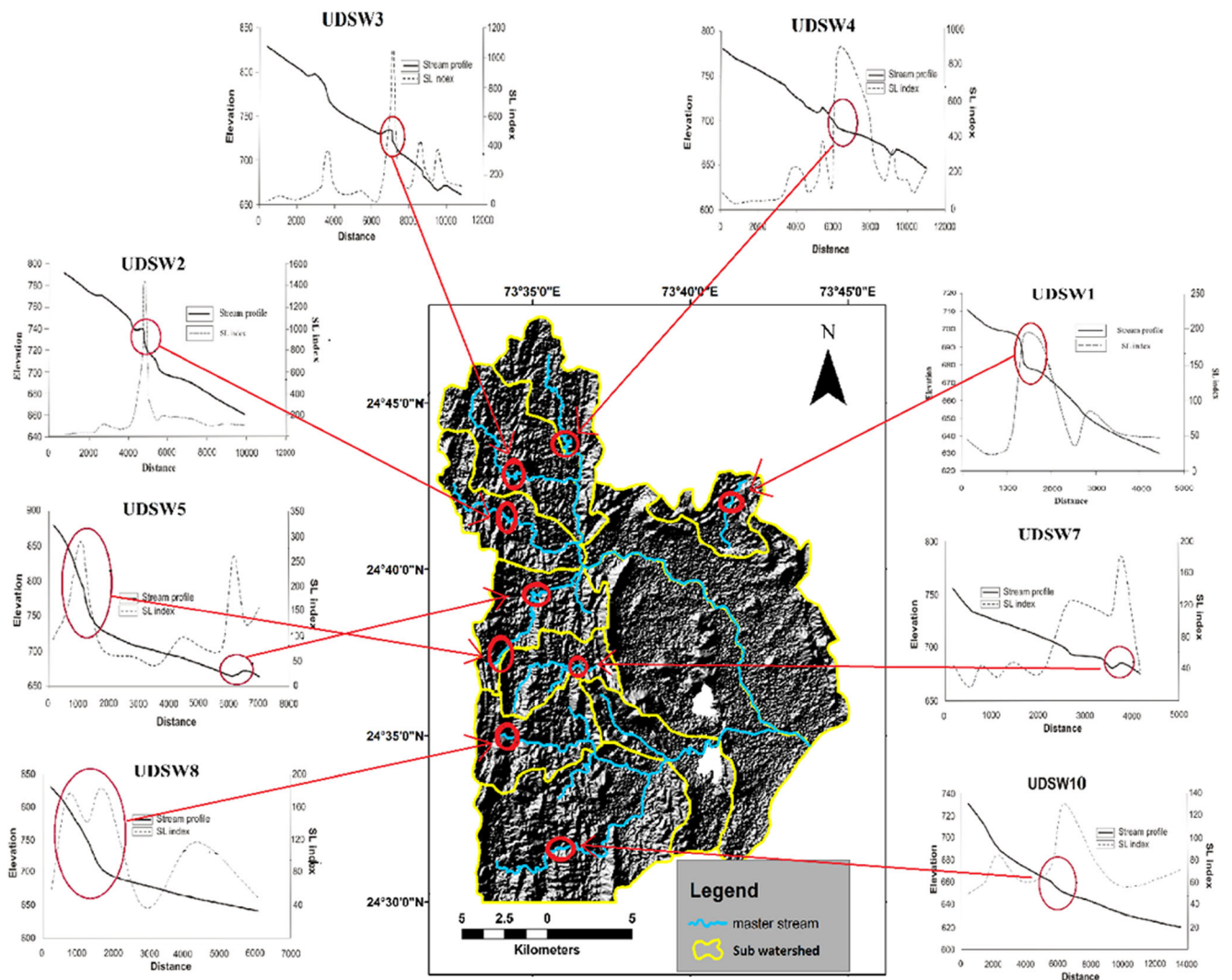
Fig. 3 Graph showing SL index with respect to stream profile and the exact position of anomalies area

just above 4 which reveals the watersheds is elongated in nature and tectonically highly active. Bs index of UDSW3 is just above 3 and falls in class 2 indicates elongated to sub-elongated in nature and tectonically moderately active. Remaining part of the study area has Bs value less than 3 or it can be say more or less close to 2, which indicates these sub watersheds show more circular in nature and tectonically less active region.

Transverse topographic symmetry factor (TTSF)

Neotectonic activity of an area can be identified by the study of drainage basin asymmetry although the active structures are poorly exposed or covered by quaternary alluvium (Cox et al. 2001). If there is no tectonic activity occurs, then the main river will flow evenly from both sides as a perfect symmetric basin, and the value of TTSF will be zero. The TTSF value varies from 0 to 1 depending upon the intensity of the tectonic activity. Values near to 1.0 indicate that the river flows closely

to the margins of the basin, a result probably produced by intensive and recent tectonic activity. Values of TTSF were calculated to assess the migration of streams perpendicular to the drainage basin axis (Keller and Pinter 1996).

The value of TTSF for all the sub-watersheds is determined, and the results are presented in Table 2. Position of the TTSF value which has been calculated is also shown (Fig. 5f). TTSF value ranges from 0.05 (almost symmetry) to 0.47 (asymmetry). Transverse topographic symmetry factor can be classified into three classes such as class 1 for TTSF > 0.4, class 2 for T between 0.2 and 0.4, and class 3 for TTSF < 0.2 ([42]). Sub-watersheds UDSW2, 3, 4, 5, and 10, situated western part of the study area, have T value more than 0.4 (Fig. 5f) showing asymmetry in nature indicates these areas are classified as tectonically active. UDSW7 and UDSW8 of the western part of the study area has TTSF value 0.18 (class 3) and 0.32 (class 2), respectively, indicating tectonically less active and moderately active. UDSW6 falls in class 2 with TTSF value 0.32, and TTSF value of UDSW1 has 0.18 and falls in class 3.
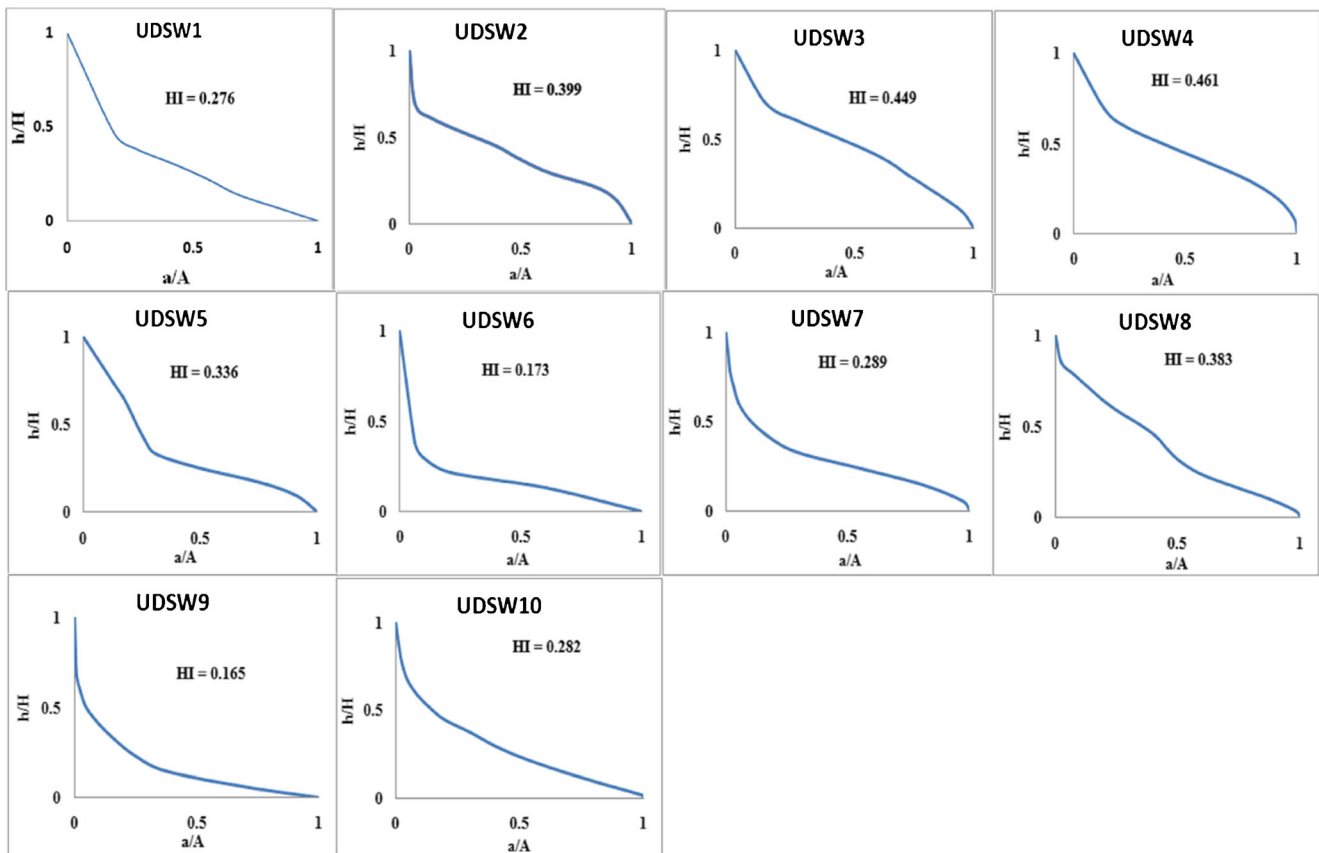
Fig. 4 Sub-watershed wise hypsometric curve, where h/H is the relative height and a/A is the relative area

Stream deflection

Sudden change of stream flow direction is stream anomaly that occurs due to tectonic structural elements such as fault or fold or may be due to lithological change. Thus stream network analysis is a fundamental tool in tectonic geomorphology (Deffontaines and Chorowich 1991; Malik and Nakata 2003; Matsuda 1975; Matsuda 1966). Defflection of stream course occurs when it crosses through fault zone because the variation of erosion took place in fault zone.

Encircled areas are showing anomalies, i.e., deflection of the flow direction of stream course (Fig. 6b). In the encircled area of sub-watershed UDSW10 at intersection with fault, stream course changed its direction from SE to NE with angle of 85°. In the area A3 and A4, the stream flows towards NNE and suddenly changed its direction towards NE and towards east making angle 65° and 70°, respectively. At point encircled, A1 stream changed its direction from SE to east with an angle 67°. In the area A2, stream flow towards south parallel to mountain front and changed its direction and suddenly changed its direction with 120° and moves towards NE along the Chambal-Jamnagar lineament. Interestingly 3.8 Km apart from the point of deflection towards NE (same direction of the stream after changed its direction), there is a fault and the trend of the fault is NE-SW. Encircled A2 and A3 shows

after deflection that the stream moves towards NE and making nearly linear or curvilinear with the fault.

Lineament

Lineament mapping is a valuable component to understand the tectonic behavior of the area (Kassou et al. 2012). Dominant lineament direction can give the idea about the regional fracture pattern of an area (McElfresh et al. 2002; Casas et al. 2000; Aldharab et al. 2018a, b). Linear geological structures of seismogenic compressional setting were identified through false color composite (FCC), edge enhancement filters, and DEM-derived product to understand tectonic behavior of the area and evaluate the compressional direction (Ali and Ali 2017). The high-density lineament was observed towards western side of the area (Fig. 7a). Rose diagram shows the orientation of lineament distribution of the area (Fig. 7b). The main direction is N-S followed by NE-SW and NW-SE. Small amount of E-W direction is also present. The lineament map also indicates that the present day stream network is influenced by the lineament direction (Fig. 7c).

Dassarma (1988) assumed clockwise rotation of Aravalli orographic axis. According to Roy and Jakhar (2002), rotational movement during neotectonic transverse to the Aravalli
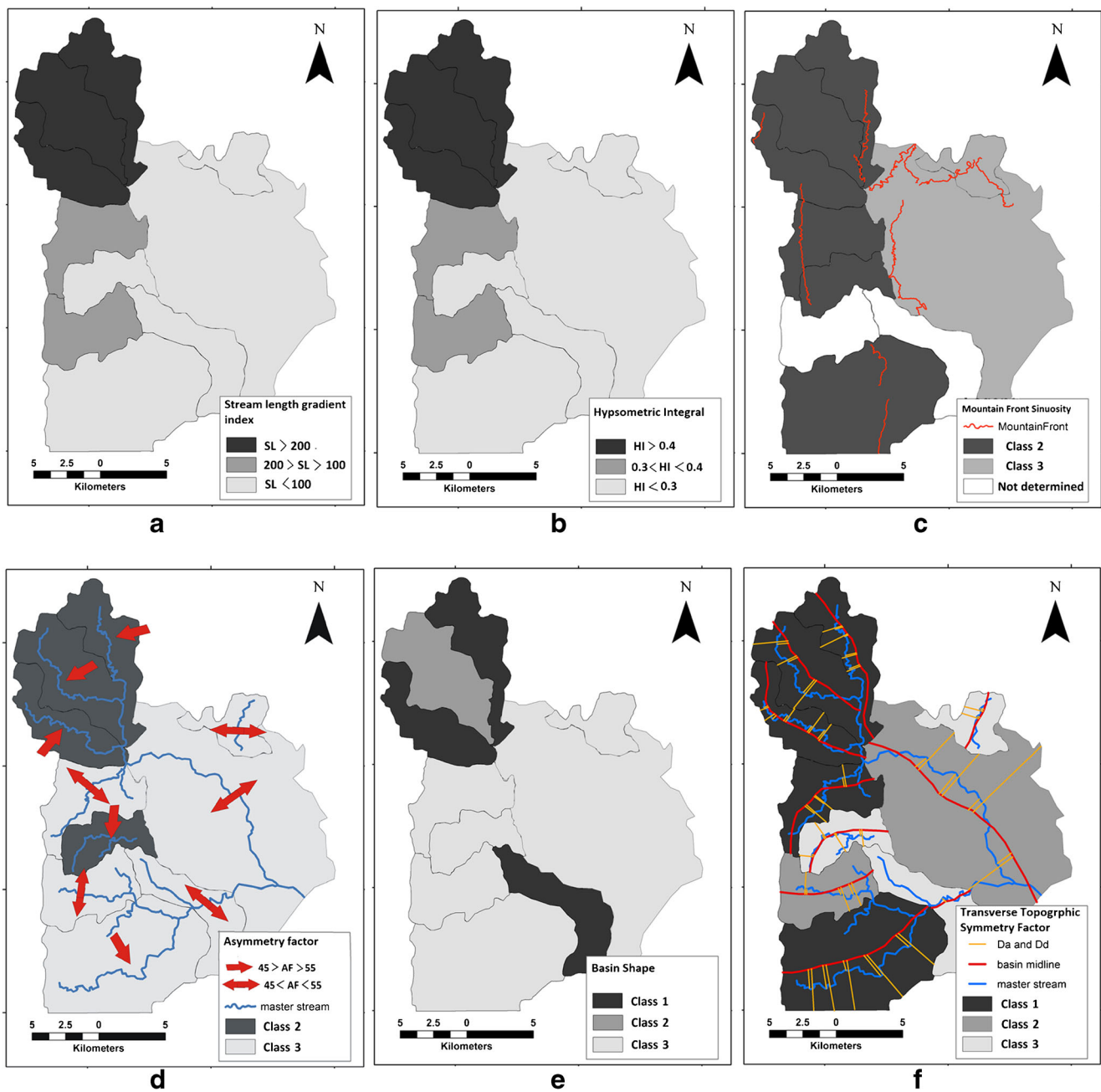
Fig. 5 Classification based on different geomorphic indices (**a**) SL index, (**b**) HI index, (**c**) Smf, (**d**) AF, (**e**) Bs, and (**f**) T

orographic axis between the Sambhar lake and the Kantli river where a series of N-S, NW-SE, and NE-SW faults intersects each other and a number of saline lake including Sambhar and Jinmata have been formed due to the development of marginal depression in the eastern fringes by the help of those rotational process. Near Jaipur, a large-scale conjugate fault set with strike of NE-SW and NW-SE, caused rotation and tilting of rock units besides considerable strike slip movement, indicates their displacement caused by recent north-south-directed maximum stress (Das 1988), and this stress developed due to the movement of Udaipur block towards north-

east direction at the rate of 49 mm per year (Bhu et al. 2014). Ghosh et al. (1991) demonstrated post-Neogene reactivation of earlier strike slip faults based on the presence of a set of regularly spaced WSW-ENE trending cross fractures affecting the quaternary deposits and the basement rocks in the central part of Aravalli mountain. These fractures along with another set of SSE-NNW strike slip faults are responsible for the development of push-up swells and grabens as two major morphotectonic features. Bundelkhand wedge penetrate the Aravalli orogen from the east and Great Boundary Fault (GBF) representing a major dislocation zone in eastern
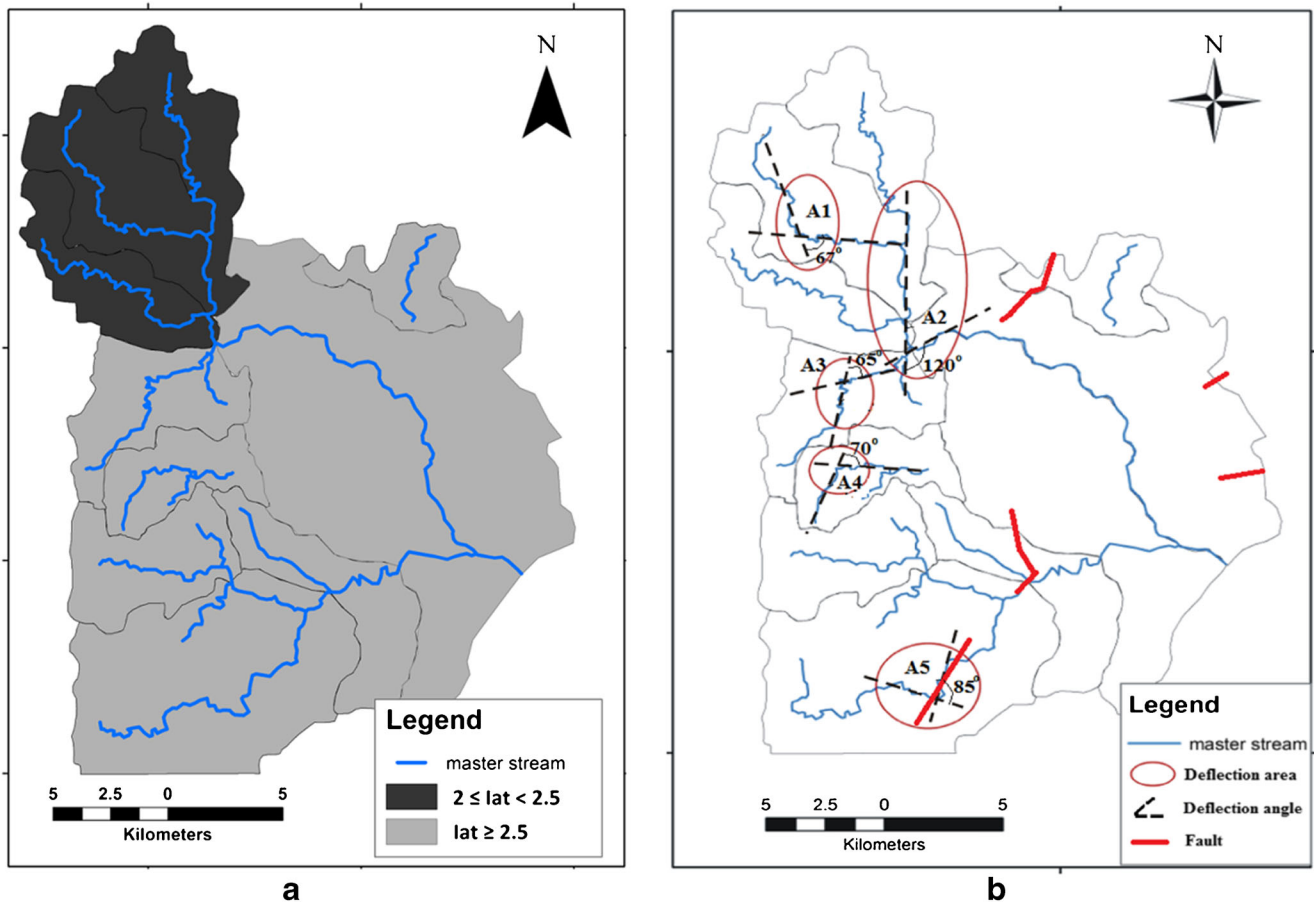
Fig. 6 (**a**) Relative tectonic activity, (**b**) stream deflection

Rajasthan. Rejuvenation of older NW-SE and NE-SW faults and formation of E-W grabens are the results of N-S compressive stress which were generated by Neogene indentation process (Sinha-Roy 1986).
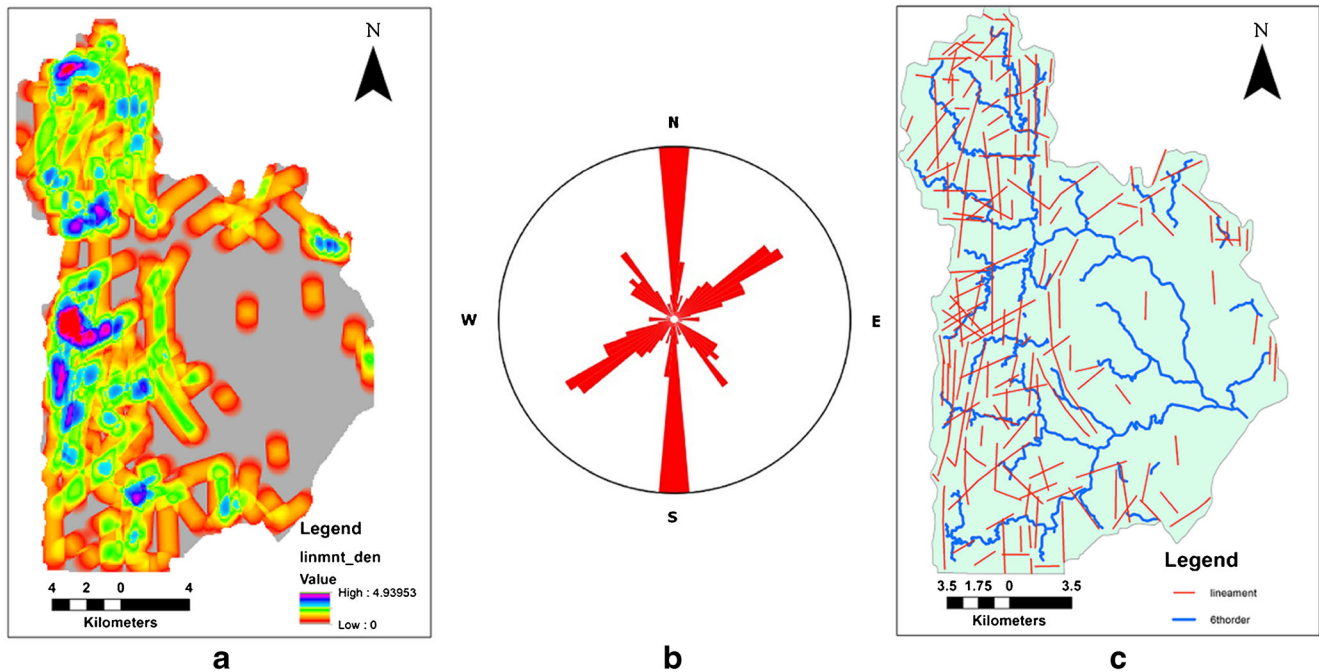

Fig. 7 Lineament map (**a**) density of lineament, (**b**) rose diagram shows orientation of lineament, and (**c**) lineament map with master stream network

Geomorphic response of active tectonics

Abundant evidence of vertical displacement and rock deformations observed here, but interpretation of active tectonic is difficult due to lack of absolute date of displacement. Mainly Archean and Proterozoic rocks covered the whole area, but quaternary and recent alluvium overlies in isolated patches, along river courses and in the shallow depressions (CGWB report, 2013). A major crack of NW-SE orientation has been found in the field but did not identify the movement (Fig. 8a). In zoom in position of that figure, no vegetation and truncated

roots are observed along the crack indicates that the crack has been developed recently after plantation. Abrupt deflection of river channel of nearly right angle (Fig. 8b) flowing from SSW to east on phyllitic rock, straight river course (Fig. 9a) of Kotra Nadi flowing towards east, displacement and movement of lineament (Fig. 9c), and straight mountain front (Fig. 9d) are some evidences that express as active tectonic. Figure 9b shows straight river course following NE-SW Chambal-Jamnagar lineament. At the position of yellow circle, the rock is composed of phyllite and schist of Jharol group, and the river got high meandering where N-S trending
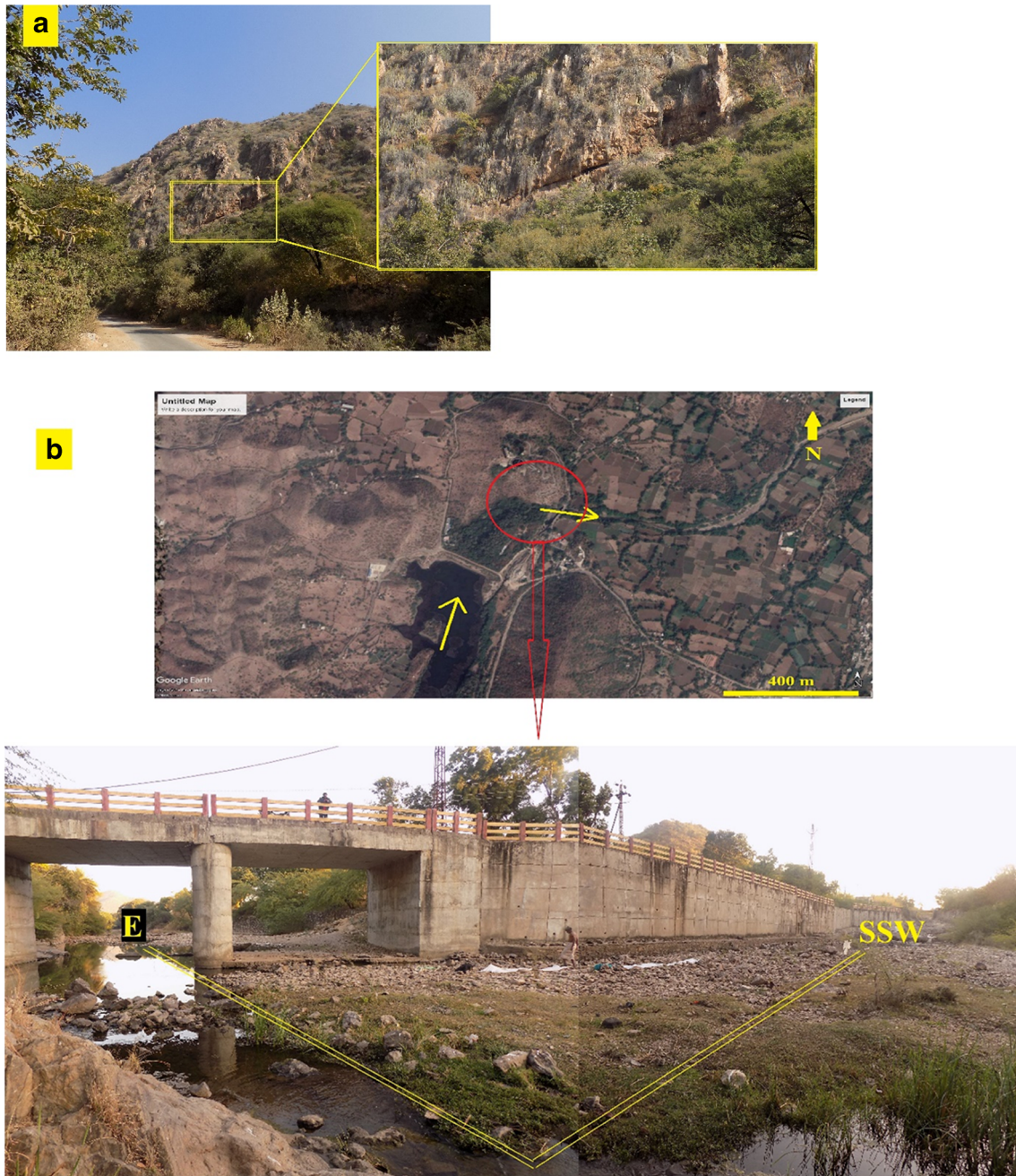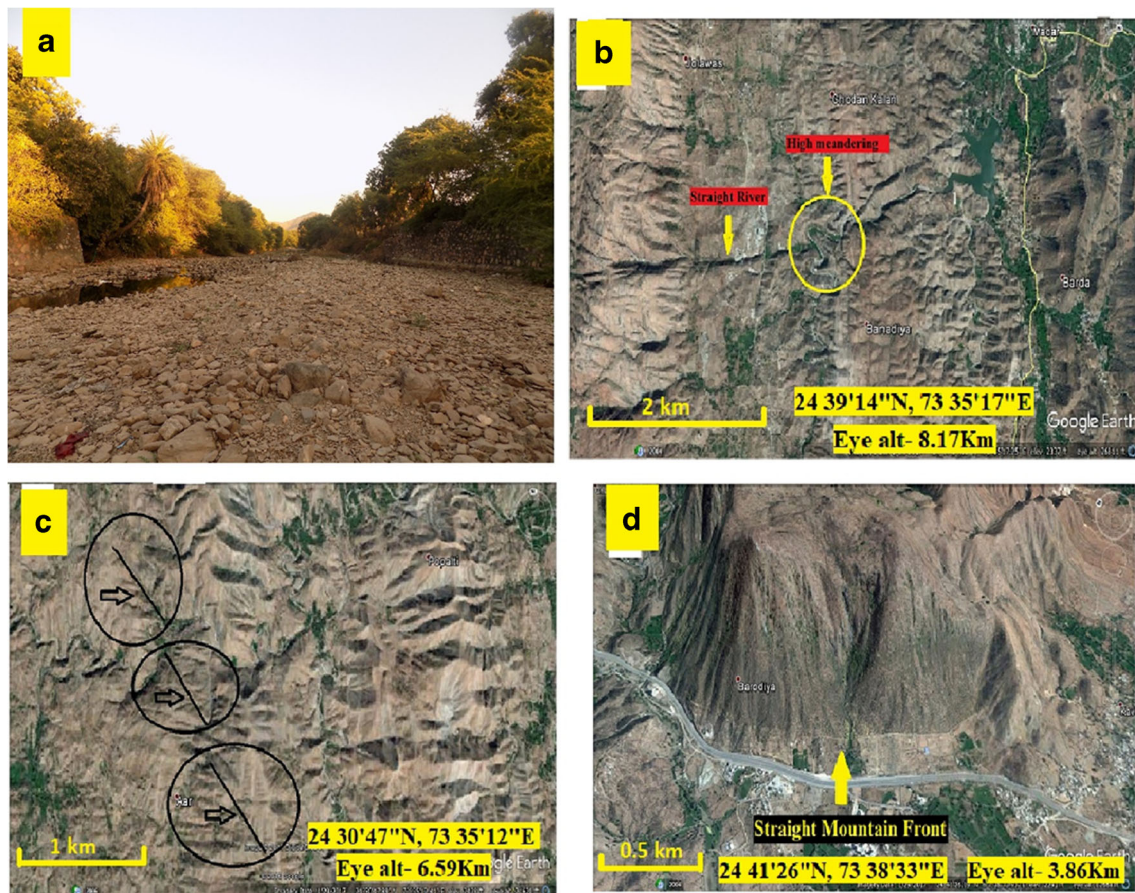

Fig. 8 Field evidences of active tectonics

Fig. 9 Field evidences of active tectonics

lineament crosscut the Chambal-Jamnagar lineament. The western part of the study area is more elevated as compared to eastern side (Fig. 1b).

Discussion

Conventional morphometric analyses of an area in Kachchh bounded by North Wagad Fault (NWF) and the Gedi fault (GF) zones suggested that the past and current seismicity is associated with both the NWF and GF (Bhattacharya et al. 2013). Identification of a number of active fault was done on the basis of filed (both geological and geophysical) investigation and satellite photo interpretation, which suggested imprints of Holocene to post-Tertiary tectonic activity along fault (Mathew et al. 2006; Patidar et al. 2008; Rajendran et al. 2008; Maurya et al. 2013; Chowksey et al. 2011; Bhattacharya et al. 2013; Kothyari et al. 2016a, b, c). Sareen et al. (1993) worked on Sabarmati river and showed that the flow has deviated from the regional slope due to middle to late quaternary neotectonism. GPS study (2009–2015) in Kachchh reveals that very low amount of intraplate deformation mainly happened in weak zone where earthquake may trigger due to combination of local and regional stress (Dumka et al.

2019). The movement of Udaipur block has already measured by Bhu et al. (2014), suggesting the present study area is tectonically active. Geomorphic indices were used to assess relative index of active tectonics (RIAT) along E-W-trending Kachchh Mainland Fault (KMF), which suggest that the central and eastern segment of KMF are tectonically more active as compare to western segment (Prizomwala et al. 2016). Evaluation of neotectonic activity along 100-Km long ENE-WSW-trending Narmada-Son Fault (NSF) has been done based on geomorphic indices and DEM analysis, where the study area was divided into four morphotectonic segments (segment I to IV) whereas segment II has undergone the highest intensity of neotectonic activity (Joshi et al. 2013). Morphometric analysis of Madhumati watershed was done with the help of various geomorphic parameters and suggested that the area is tectonically active (Bali et al. 2016).

WNW-ESE and NE-SW lineament are more persistent pairs of lineaments that developed in Rajasthan and Gujarat, originated later than early-middle Jurassic and have maximum control in the evolution of quaternary landforms (Bhu et al. 2014; Roy and Jakhar 2002). This ancient and neotectonically active lineament has a great importance of seismic activity. Epicenter of these earthquake located on both the

Table 3   Relative tectonic activity classification

Sub-watershed	Area (Km2)	SL	Vf	Smf	Hi	Af	Bs	T	Iat = S/n	Iat class
UDSW1	15.72	3	3	3	3	3	3	3	3	4
UDSW2	25.61	3	3	2	2	2	1	1	2	3
UDSW3	36.94	3	3	2	2	2	2	1	2.14	3
UDSW4	27.34	3	3	2	2	2	1	1	2	3
UDSW5	27.95	3	3	3	2	3	3	1	2.57	4
UDSW6	153.30	3	–	3	3	3	3	2	2.83	4
UDSW7	19.04	3	3	3	2	2	3	3	2.71	4
UDSW8	27.19	3	3	3	–	3	3	2	2.83	4
UDSW9	27.78	3	3	3	–	3	1	3	2.67	4
UDSW10	76.43	3	3	3	–	3	3	1	2.67	4

Precambrian lineament and NW-SE trending quaternary lineament due to the Indian plate collision which suggests intraplate deformation in the Aravalli craton (Bhu et al. 2014).

In this present paper, various geomorphic indices were used to understand the relative tectonic activity of the area. Based on the average value of SL and Vf, all the sub-watersheds fall in class 3 indicates the whole area is tectonically less active or stable, but in some places, highly fluctuation of river gradient (even some places SL value more than 1000) and "V" shape valley (sometime Vf is less than 0.5) are the imprints of neotectonism mainly observed in the western part of the study area. UDSW 2, 3, 4, and 8 shows convex upward hypsometric curve along with high hypsometric integral indicates active upliftment in the northwestern and small portion of western part of the study area. Smf value of individual mountain front shows that few mountain front belonging to UDSW 2, 5, and 10 are straight (low Smf value) indicates the area is relatively more active. The AF and TTSF value shows that the northwestern part and the western part of the study area are affected by river migration and tectonic tilting. After combination of all the geomorphic parameters, the relative index of active tectonics suggests that the northwestern flank of the study area is tectonically moderately active whereas the remaining part of the area is considered as partially stable. Lineament study, stream deflection along with some field evidences also supports the results of above geomorphic indices.

Discussion of relative tectonic activity (RIAT)

Several studies explained relative tectonic activity of mountain front by using only two geomorphic index (Smf and Vf). The Vf values are plotted with the Smf values on the same diagram in order to produce a relative degree of tectonic activity and recognition of three different classes by describing "active front" having Smf and Vf value is less than 1.6 and less than 0.5, respectively (Bull and McFadden 1977; Silva et al. 2003). Aravalli is an example of mountain under erosion. Geomorphic indices such as SL, Vf, Smf, HI, Af, Bs, and T

has been applied to evaluate RIAT. Every geomorphic index has been classified into three classes in which class 1 and class 3 represents high and low tectonically active respectively. Relative index of active tectonics (RIAT) is obtained by the average of the different classes of geomorphic indices (S/n) and classified into four classes, where class 1 is very high tectonic activity with values of S/n between 1 and 1.5; class 2 is high tectonic activity with values of $1.5 \leq S/n < 2$; class 3 is moderately active tectonics with $2 \leq S/n < 2.5$; and class 4 is low active tectonics with values of $S/n \geq 2.5$ (El Hamdouni et al. 2008).

The RIAT values are summarized in Table 3. On the basis of RIAT index, sub-watersheds UDSW2, UDSW3, and UDSW4, occupying 20.56% of the total area, are fall in class 3, which reveals that northwestern part of the study area shows moderately tectonic activity, whereas the rest of the study area, i.e., 79.44% of the total area, where RIAT index is class 4, considered as partially stable area (Fig. 6a).

Conclusion

• Based on calculated RIAT values nearly one third of the area falls in class 3 indicate moderate tectonic activity, found in northwestern part of the study area.

• High value of HI, Bs are observed, which can be attributed to the presence of fault and fold in the area.

• Presence of prominent fault of tectonic origin, abrupt change of stream direction, major crack, sudden river meandering, straight mountain front, etc. corresponds to the class 3 ,i.e., moderately active.

• The Smf value suggests that the mountain front of northwestern flank are tectonically active in nature.

• Vf value suggests low rate of incision associated with tectonic uplift.

• The results of present study confirm the applicability of RIAT calculation by using geomorphic indices for assessing tectonic activity.

References

Ahmad S, Bhat MI (2013) Investigating drainage response to the Balapur fault interaction on the north eastern Pir Panjal flank, Kashmir valley, India. J Himalayan Ecol Sustain Dev 8:121–137

Aldharab HS, Ali SA, Ikbal J, Ghareb S (2018a) GIS and hypsometry based analysis on the evolution of sub-basins in Ataq area-Shabwah, Yemen. Int J Res Appl Sci Eng Technol 6:3489–3497

Aldharab HS, Ali SA, Ikbal J, Ghareb S (2018b) Spatial analysis of lineament and their tectonic significance using Landsat imagery in Alarasah area- southeastern Central Yemen. J Geogr Environ Earth Sci Int 18(2):1–13

Ali SA, Ali U (2017) Evaluating linear geological structures in seismogenic compressional setting, Kashmir basin, NW-Himalaya. Spat Inf Res 25(6):801–811

Ali U, Ali SA (2018) Seismically induced soft-sediment deformation structures in an active seismogenic setting: the Plio-Pleistocene Karewa deposits, Kashmir Basin (NW Himalaya). J Struct Geol 115:28–46

Ali SA, Ikbal J, Ali U, Aldharab HS (2017) Measurement of watershed geometry in the central part of Udaipur sector, Rajasthan using remote sensing and GIS. Int J Rec Sci Res 8(11):21786–21791

Azor A, Keller EA (2002) Yeats, R.S. geomorphic indicators of active fold growth: oak ridge anticline, Ventura basin, southern California. GSA Bull 114:745–753

Bakliwal PC, Ramasamy SM (1987) Lineament fabric of Rajasthan and Gujarat. Geol Surv India 113(7):54–64

Bali BS, Wani AF, Khan RA, Ahmad S (2016) Morphotectonic analysis of the Madhumati watershed, Northeast Kashmir Valley. Arab J Geosci 9:390–317. https://doi.org/10.1007/s12517-016-2395-9

Bathrellos GD, Antoniou VE, Skilodimou HD (2009) Morphotectonic characteristics of Lefkas Island during the quaternary (Ionian Sea, Greece). Geol Balcanica 38:23–33

Bhattacharya F, Rastogi BK, Kothyari G (2013) Morphometric evidence of seismicity around the Wagad and Gedi faults, eastern Kachchh, Gujarat , India. J Geol Soc India 81:113–121

Bhu H, Purohit R, Ram J, Sharma P, Jakhar SR (2014) Neotectonic activity and parity in movements of Udaipur block of the Arvalli Craton and Indian plate. J Earth Syst Sci 123(2):343–350

Bull PA (1977) Glacial deposits identified by chattermark trails in detrital garnets - comment. Geology 5:248–49

Bull WB (1978) Geomorphic tectonic classes of the south front of the San Gabriel Mountains, California. U.S. Geological Survey Contract Report, 14–08-001-G-394, Office of Earthquakes, Volcanoes and Engineering, Menlo Park, Calif, 59

Bull WB (2007) Tectonic geomorphology of mountains: a new approach to Paleoseismology, vol 328. Wiley-Blackwell, Oxford

Bull W, McFadden L (1977) Tectonic geomorphology north and south of the Garlock fault, California. In: Doehring DO (ed) Geomorphology in arid regions. State University of New York at Bingamton, Geomorphology, pp 115–138

Burbank DW, Anderson RS (2001) Tectonic geomorphology, vol 247. Blackwell Science, Oxford

Casas AM, Cortes AL, Maestro A, Soriano MA, Riaguas A, Bernal JA (2000) Program for lineament length and density analysis. Comput Geosci 26(9/10):1011–1022

Chen YC, Sung QC, Cheng KY (2003) Along-strike variations of morphotectonic features in the western foothills of Taiwan: tectonic implications based on stream gradient and hypsometric analysis. Geomorphology 56:109–137

Chowksey V, Maurya DM, Joshi J, Khonde N, Das A, Chamyal LS (2011) Lithostratigraphic development and neotectonic significance of the quaternary sediments along the Kachchh mainland fault (KMF) zone, Western India. J Earth Syst Sci 120(6):979–999

Cox RT (1994) Analysis of drainage basin symmetry as a rapid technique to identify areas of possible quaternary tilt block tectonics: an example from the Mississippi embayment. Geol Soc Am Bull 106: 571–581. https://doi.org/10.1130/00167606(1994)106<0571:AODBSA>2.3.CO;2

Cox RT, Van Arsdale RB, Harris JB (2001) Identification of possible quaternary deformation in the northwestern Mississippi embayment using quantitative geomorphic analysis of drainage basin asymmetry. Geol Soc Am Bull 113:615–624

Das AR (1988) Geometry of superposed deformation in the Delhi Supergroup of rocks of the area around Bhabru Manoharpura, district Jaipur, Rajasthan. Unpublished Ph.D thesis, University of Rajasthan, Jaipur, 116

Dassarma DC (1988) Post-orogenic deformation of the Precambrian crust in Northeast Rajasthan. In: Roy AB (ed) Precambrian of Aravalli mountain, Rajasthan, India, Mem. Geol. Soc. India, vol 7, pp 109–120

Deffontaines B, Chorowich J (1991) Principle of drainage basin analysis from multisource data: application to the structural analysis of the Zaire basin. Tectonophysics 194:237–263

Demoulin A (1998) Testing the tectonic significance of some parameters of longitudinal river profiles: the case of the Ardenne (Belgium, NW Europe). Geomorphology 24(2):189–208

Dubey RK, Dar JA, Kothyari GC (2017) Evaluation of relative tectonic perturbations of the Kashmir basin, northwest Himalaya, India: an integrated morphological approach. J Asian Earth Sci 148:153–172

Dumka RK, Chopra S, Prajapati S (2019) GPS derived crustal deformation analysis of Kachchh, zone of 2001(M7.7) earthquake, Western India. Quat Int. https://doi.org/10.1016/jquaint.2019.01.032

El Hamdouni R, Irigaray C, Fernández T, Chacón J, Keller EA (2008) Assessment of relative active tectonics, southwest border of Sierra Nevada (southern Spain). Geomorphology 96:150–173. https://doi.org/10.1016/j.geomorph.2007.08.004

Elias Z (2015) The neotectonic activity along the lower Khazir River by using SRTM image and geomorphic indices. Earth Sci 1(1):50–58. https://doi.org/10.11648/j.earth.20150401.15

Gaidzik K, Ramírez-Herrera MT (2017) Geomorphic indices and relative tectonic uplift in the Guerrero sector of the Mexican forearc. Geosci Front 8:885–902

Ghosh TK, Viswanathan S, Suval B (1991) Neotectonic analysis of Medha river basin, Rajasthan, India. Int. jour. Remote Sens 12: 2585–2595

Hack JT (1973) Stream-profiles analysis and stream-gradient index. Journal of research of the U.S. Geol Survey 1(4):421–429

Hare PW, Gardner TW (1985) Geomorphic indicators of vertical neotectonism along converging plate margins, Nicoya Peninsula, Costa Rica. In Tectonic Geomorphology, Morisawa, M., Hack, J.T., Eds.; Proceedings of the 15th Annual Binghamton Geomorphology Symposium. Allen and Unwin, Boston, 123–134

Heron AM (1936) The geology of south eastern Mewar. Mem Geol Surv India 68(1):1–120

Huang XJ, Niemann JD (2006) Modelling the potential impacts of groundwater hydrology on long-term drainage basin evolution. Earth Surf Process Landf 31:1802–1823

Ikbal J (2018) Structural and tectonic study of Aravalli Supergroup in the central part of Udaipur sector, Rajasthan using geological and geospatial techniques. Doctoral thesis, Aligarh Muslim university

Ikbal J, Ali SA (2017) Site selection for soil conservation by geometric analysis of watershed, southeastern part of Aravalli mountain range using remote sensing and GIS. Int J Sci Res Sci Technol 8:369–378

Ikbal J, Ali SA, Aldharab H (2017) Morphological character of micro watershed of Katla river in Udaipur district, Rajasthan. Int J Curr Res 9(9):57708–57715

Joshi PN, Maurya M, Chamyal LS (2013) Morphotectonic segmentation and spatial variability of neotectonic activity along the Narmada–son fault, Western India: remote sensing and GIS analysis. Geomorphology 180-181:292–306

Kamberis E, Bathrellos GD, Kokinou E, Skilodimou HD (2012) Correlation between the structural pattern and the development of the hydrographic network in a portion of the Western Thessaly Basin (Greece). Cent Euro J Geosci 4(3):416–424

Kassou A, Essahlaoui A, Aissa M (2012) Extraction of Structural Lineaments from Satellite Images Landsat7 ETM+ of Tighza Mining District (Central Morocco) Research. J Earth Sci 4(2):44–48

Kele VS, Sengupta S, Achyuthan H, Jaiswal MK (2014) Tectonic controls upon Kaveri River drainage, cratonic peninsular India: inferences from longitudinal profiles, morphotectonic indices, hanging valley and fluvial records. Geomorphology 227:153–165

Keller EA (1986) Investigation of active tectonics: use of surficial Earth processes. In: Wallace RE (ed) Active Tectonics, Studies in Geophysics. National Academy Press, Washington, DC, pp 136–147

Keller EA, Pinter N (1996) Active tectonics: earthquakes, uplift, and landscape. Prentice hall, Inc, New Jersey, pp 121–205

Kothyari GC (2015) Morphometric analysis of tectonically active Pindar and Saryu river basins: central Kumaun Himalaya. Z Geomorphol 59(4):421–442

Kothyari GC, Dumka RK, Singh AP, Chauhan G, Thakkar MG, Biswas SK (2016a) Tectonic evolution and stress pattern of south Wagad fault at the Kachchh Rift Basin in western India. Geol Mag. https://doi.org/10.1017/S0016756816000509

Kothyari GC, Shukla AD, Juyal N (2016b) Reconstruction of Late Quaternary climate and seismicity using fluvial landforms in Pindar River valley, central Himalaya, Uttarakhand, India. Quat Int xxx:1–17. https://doi.org/10.1016/j.quaint.2016.06.001

Kothyari GC, Rastogi BK, Morthekai P, Dumka RK (2016c) Active segmentation assessment of the tectonically active south Wagad fault in Kachchh, Western peninsular India. Geomorphology 253:491–507

Mahmood SA, Gloaguen R (2012) Appraisal of active tectonics in Hindu Kush: insights from DEM derived geomorphic indices and drainage analysis. Geosci Front 3(4):407–428. https://doi.org/10.1016/j.gsf.2011.12.002

Malik JN, Mohanty C (2007) Active tectonic influence on the evolution of drainage and landscape: geomorphic signatures from frontal and hinterland areas along the northwestern Himalaya, India. J Asian Earth Sci 29:604–618. https://doi.org/10.1016/j.jseaes.2006.03.010

Malik JN, Nakata T (2003) Active faults and related and late quaternary deformation along the northwestern Himalayan frontal zone, India. Ann Geophys 46(5):917–936

Mathew G, Singhvi AK, Karanth RV (2006) Luminescence chronometry and geomorphic evidence of active fold growth along the Kachchh mainland fault (KMF), Kachchh, India: Seismotectonic implications. Tectonophys 422:71–87

Matsuda T (1966) Strike-slip faulting along the Atotsugawa fault, Japan. Bull Earthq Res Instit 44:1179–1212

Matsuda T (1975) Active fault assessment for Irozaki fault system, Izu Peninsula. In: Tsuchi R (ed) Reports on the earthquake of Izu peninsula, 1974, and the disaster. The Ministry of Education, Tokyo, pp 121–125

Maurya DM, Chouksey V, Joshi PN, Chamyal LS (2013) Application of GPR for delineating the neotectonic setting and shallow subsurface nature of the seismically active Gedi fault, Kachchh, western India. J Geophys Eng 10:034006. https://doi.org/10.1088/1742-2132/10/3/034006

McElfresh SBZ, Harbert W, Ku CY (2002) Lin, J.S. stress modeling of tectonic blocks at Cape Kamchatka, Russia using principal stress proxies from high-resolution SAR: new evidence for the Komandorskiy block. Tectonophysics 354:239–256

Moglen GE, Bras RL (1995) The effect of spatial heterogeneities on geomorphic expression in a model of basin evolution. Water Resour Res 31:2613–2623

Molin P, Pazzaglia FJ, Dramis F (2004) Geomorphic expression of active tectonics in a rapidly-deforming forearc, Sila massif, Calabria, southern Italy. Am J Sci 304(7):559–589

Özkaymak Ç (2015) Tectonic analysis of the Honaz fault (western Anatolia) using geomorphic indices and the regional implications. Geodin Acta 27(2–3):110–129. https://doi.org/10.1080/09853111.2014.957504

Patidar AK, Maurya DM, Thakkar MG, Chamyal LS (2008) Evidence of neotectonic reactivation of the Katrol Hill fault during late quaternary and its GPR characterization. Curr Sci 94:338–346

Pedrera A, Galindo-Zaldívar J, Ruíz-Constan A, Duque C, Marín-Lechado C, Serrano I (2009) Recent large fold nucleation in the upper crust: Insight from gravity, magnetic, magnetotelluric and seismicity data (Sierra de Los Filabres-Sierra de Las Estancias, Internal Zones, Betic Cordillera). Tectonophysics 463:145–160. https://doi.org/10.1016/j.tecto.2008.09.037

Pike RJ, Wilson SE (1971) Elevation-relief ratio, hypsometric integral, and geomorphic area-altitude analysis. Bulletin of the Geological Society of America 82(4):1079–1084. https://doi.org/10.1130/0016-7606(1971)82[1079:ERHIAG]2.0.CO;2

Prizomwala SP, Solanki T, Chauhan G, Das A, Bhatt N, Thakkar MG, Rastogi BK (2016) Spatial variations in tectonic activity along the Kachchh mainland fault, Kachchh, western India: implications in seismic hazard assessment. Nat Hazards 82:947–961. https://doi.org/10.1007/s11069-016-2228-x

Rajendran CP, Rajendran K, Thakkar M, Goyal B (2008) Assessing the previous activity at the source zone of the 2001 Bhuj earthquake based on the near-source and distant paleo-seismological indicators. J Geophys Res 113:B05311. https://doi.org/10.1029/2006JB004845

Riquelmea R, Martinod J, Herail G, Darrozesa J, Charrierb RA (2003) Geomorphological approach to determining the Neogene to recent tectonic deformation in the coastal cordillera of northern Chile (Atacama). Tectonophysics 361:255–275

Rockwell TK, Keller EA, Johnson DL (1985) Tectonic geomorphology of alluvial fans and mountain fronts near Ventura, California. In Tectonic Geomorphology, Morisawa, M., Eds.; Proceedings of the 15th Annual Geomorphology Symposium. Allen and Unwin Publishers, Boston, MA, 183–207

Roy AB, Jakhar SR (2002) Geology of Rajasthan (Northwest India) Precambrian to recent, vol 349. Scientific publishers, Jodhpur

Saifuddin I (2000) Thrust controlled lineaments of the Aravalli-Delhi fold belt, Rajasthan, India mapped from Landsat TM image. J Indian Soc Remote Sens 28:47–58

Sareen BK, Tandon SK, Bhola AM (1993) Slope-deviatory alignment, stream network and lineament orientation of the Sabarmati River

system—neotectonic activity in the mid-to late quaternary. Curr Sci 64:827–836

Schumm SA (1977) The fluvial system, vol 338. Wiley, New York

Siddiqui S (2014) Appraisal of active deformation using DEM-based morphometric indices analysis in Emilia-Romagna Apennines, Northern Italy. Geodyn Res Int Bull 1(3):XXXIV–XXLII

Silva PG, Goy JL, Zazo C, Bardaji T (2003) Fault generated mountain fronts in south-east Spain: Geomorphologic assessment of tectonic and seismic activity. Geomorphology 50:203–225. https://doi.org/10.1016/S0169-555X(02)00215-5

Sinha-Roy S (1986) Himalayan collision and indentation of Aravalli orogen by Bundelkhand wedge: implication for Neotectonics in Rajasthan. Proc international symposium on Neotectonics in South Asia, Dehradun, India. 18-21

Strahler AN (1952) Hypsometric (area-altitude) analysis of erosional topology. Geol Soc Am Bull 63(11):1117–1142

Toudeshki VH, Arian M (2011) Morphotectonic analysis in the Ghezel Ozan River basin, NW Iran. J Geogr Geol 3:258–260

Whipple KX, Di-Biase RA, Crosby BT (2013) Bedrock Rivers. Treat Geomorphol 9:550–570

Whittaker AC (2012) How do landscapes record tectonics and climate? Lithosphere 4:160–164

Willgoose HG (1998) Revisiting the hypsometric curve as an indicator of form and process in transport-limited catchment. Earth Surf Process Landf 23:611–623